ORGANOMETALLICS

ARTICLE

pubs.acs.org/Organometallics

Structure and Reactivity of Acetylene Complexes of Bis(imino)pyridine Ruthenium(0)

Noah L. Wieder, Patrick J. Carroll, and Donald H. Berry*

Department of Chemistry, University of Pennsylvania, Philadelphia, Pennsylvania 19104-6323, United States

Supporting Information

ABSTRACT: Reaction of the low-valent ruthenium complex [κ^2-N_3]Ru(η^6-MeC_6H_5) (**1**), [N_3] = 2,6-(MesN=CMe)$_2$-C_5H_3N, with acetylene leads to the displacement of toluene and formation of the monoacetylene adduct, [N_3]Ru(C_2H_2) (**2**). The short alkyne−metal distances in **2** are consistent with 4 e^- donation to the metal; that is, there is some degree of overlap of the perpendicular alkyne π- and metal d_{xz}-orbitals. The NMR data and DFT calculations suggest $\pi_\perp$ donation is weaker in **2** than in many 4 e^- donor alkyne complexes. Further reaction of **2** with acetylene leads to catalytic cyclotrimerization and release of benzene, although the catalyst is short-lived. In the case of diphenylacetylene, two molecules of C_2Ph_2 react per molecule of **1** to generate the metallacyclic [N_3]Ru(C_4Ph_4) (**3**), which is best described as a ruthenacyclopentadiene, or ruthenole. Compound **3** does not react further with diphenylacetylene, but does react with terminal alkynes by addition of the acetylenic C−H bond across a ruthenole Ru−C bond. The new complexes, [N_3]Ru(C≡C-R)(*cis*,*cis*-1,2,3,4-tetraphenylbutadienyl-μ-H) (R = H, **5**; Ph, **6**), contain terminal acetylide and *cis*,*cis*-tetraphenylbutadienyl ligands (Ru-$(CPh)_4$H), where the vinylic C−H bond is weakly bound to the metal through an agostic interaction. This type of ruthenole cleavage by terminal acetylenes may explain the short life of **2** as a catalyst for cyclotrimerization. The order in which HCCH and PhCCPh are introduced into the coordination sphere alters the course of the reaction: whereas isolated Ru(C_4Ph_4) metallacycle **3** is cleaved by acetylene to give **5**, preformed acetylene complex **2** reacts with diphenylacetylene to produce the free cyclization product 1,2,3,4-tetraphenylbenzene (and **3**). These observations highlight the key role of five-membered metallacycles in alkyne cyclotrimerization, as well as the importance of steric factors in these reactions. Cyclization is observed in cases where the π-system of the ruthenacyclic intermediate is accessible to an incoming alkyne, but not in cases where steric bulk hinders access.

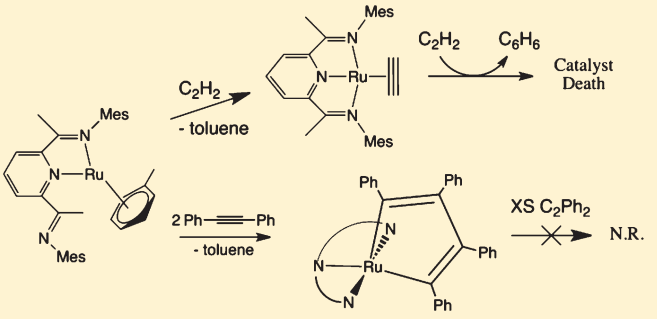

INTRODUCTION

Transition metal catalyzed formal [2+2+2] cyclotrimerization of alkynes is a reaction of considerable importance both industrially and in the laboratory.[1] Efforts to better understand this process have been well underway for at least the past three decades, and the topic has been reviewed thoroughly.[2]

The low-valent ruthenium complex [κ^2-N_3^{Ar}]Ru(η^6-MeC_6H_5) (**1**) and the bridging dinitrogen complex {[N_3^{Ar}]-Ru}$_2$(μ-N_2) ([N_3^{Ar}] = 2,6-(ArN=CMe)$_2C_5H_3N$, Ar = xylyl or mesityl) were recently described by our group.[3] Although **1** and {[N_3]Ru}$_2$(μ-N_2) are formally Ru(0) complexes, formal oxidation states often provide an incomplete description of these and other low-valent complexes bearing [N_3]-type ligands. In some instances, low-valent [N_3]M complexes are better described by canonical forms representing full transfer of one or more electrons from the metal to relatively remote ligand orbitals, e.g., $[N_3]^-/M^+$ or $[N_3]^{2-}/M^{2+}$. Previously, **1** was shown to react with various small donor ligands L (L = PMe_3, CO, C_2H_4) to yield 18-electron [N_3]RuL_2 complexes[3] and with H_2 to form an unusual paramagnetic hydride complex.[4] In the case of ethylene, the resultant [N_3]Ru$(C_2H_4)_2$ complex was not isolable, reverting to starting materials in vacuo. In this contribution we report the reactions of **1** with alkynes to form ruthenium(0) complexes [N_3]Ru(η^2-HCCR) (R = H, Me) and the ruthenium(II) metallacyclopentadiene complex [N_3]Ru(C_4Ph_4). Structural studies and the reactivity of these complexes, including catalytic cyclotrimerization of alkynes, are described.

RESULTS

Synthesis and Structure of [N_3]Ru(C_2H_2), 2. Treatment of the Ru(0) arene complex [κ_2-N_3]Ru(η^6-MeC_6H_5) (**1**) or dinitrogen complex {[N_3]Ru}$_2$(μ-N_2) with 1.3 equiv of acetylene leads to formation of the bright green acetylene complex [N_3]Ru(C_2H_2) (**2**) within minutes at room temperature (63% isolated yield, eq 1). Use of excess acetylene results in decreased yields of **2** due to byproducts generated during catalytic cyclotrimerization (vide infra). The ^{1}H NMR spectrum of **2** is consistent with C_{2v} symmetry, with a peak at δ 6.68 assigned

Received: October 1, 2010
Published: March 31, 2011

   dx.doi.org/10.1021/om100953g | *Organometallics* 2011, 30, 2125–2136

to the acetylene ligand, and no change in symmetry was observed in the ^{1}H NMR down to −68 °C. The imine methyl signal (δ 1.51) is shifted somewhat upfield compared to the free ligand (δ 2.61). A similar, albeit much greater, perturbation of the imine methyl shift (δ −0.06) is observed in the dinitrogen complex $\{[N_3]Ru\}_2(\mu\text{-}N_2)$.[3] Chirik and co-workers previously suggested that the upfield shift of the $[N_3]$ imine methyl resonances in a variety of iron(0) complexes is due to temperature-independent paramagnetism (TIP) and reflects mixing of higher spin excited states with the ground state.[5] In the ^{13}C NMR spectrum, the acetylene ligand is observed at δ 131.0 ($^1J_{CH}$ = 226.4 Hz), as assigned on the basis of a 2D-NMR experiment.

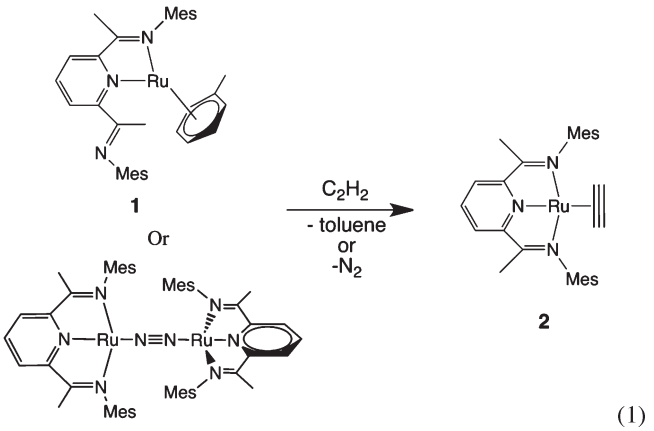

(1)

The geometry of **2** in the solid state was determined by single-crystal X-ray diffraction to be square planar, with the acetylene ligand lying within the $[N_3]Ru$ plane and coordinated trans to the pyridyl nitrogen atom (Figure 1). The coordinated C≡C bond length (1.239(4) Å) is longer by 0.06 Å compared to free acetylene (1.181(7) Å),[6] and the acetylene ligand of **2** is bound in an essentially symmetrical manner (D(Ru−C) = 2.032(2) and 2.040(2) Å). Only two other structures of mononuclear ruthenium η^2-HCCH complexes[7] were found in the Cambridge Structural Database,[8] and both can be unambiguously assigned as 2 e$^-$ donor acetylene coordinated to Ru(II) centers. Whereas the C≡C bond length of **2** is similar to these known Ru(II) acetylene complexes, the Ru−C bond lengths are ca. 0.16 Å shorter. Possible origins of the short Ru−C distances in **2** will be addressed below.

Complex **2** is stable in benzene solution indefinitely at room temperature in the absence of air and water; unlike the binuclear (μ-N_2) complex, **2** does not revert to $[\kappa^2\text{-}N_3]Ru(\eta^6\text{-}C_6H_6)$. However, dissociation of acetylene can be induced by treatment of **2** with excess CO, which leads to formation of the dicarbonyl complex $[N_3]Ru(CO)_2$ (eq 2).[3]

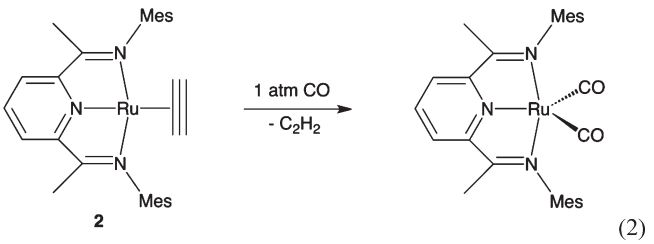

(2)

Cyclotrimerization of Alkynes Mediated by $[N_3]Ru(C_2H_2)$ and $[\eta^2\text{-}N^3]Ru(\eta^6\text{-}MeC_6H_5)$. Reaction of $[N_3]Ru(C_2H_2)$ (**2**)

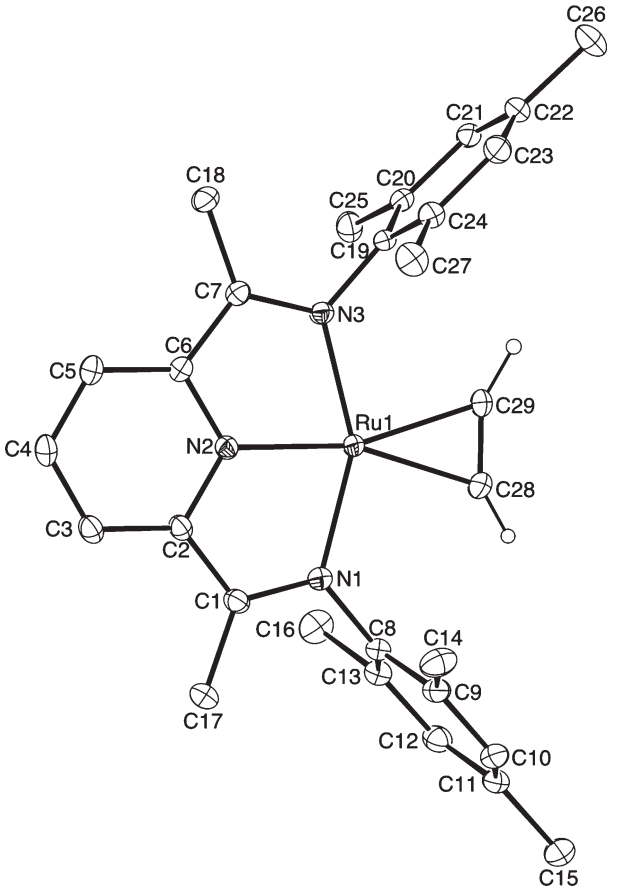

Figure 1. ORTEP drawing of $[N_3]Ru(C_2H_2)$, **2**, with 30% probability thermal ellipsoids. Selected bond lengths (Å): C28−C29, 1.239(4); Ru1−C28, 2.032(2); Ru1−C29, 2.040(2).

with 10 equiv of acetylene at room temperature in THF-d_8 leads to formation of benzene by cyclotrimerization. Not surprisingly, cyclotrimerization of acetylene is also observed in the reaction of $[\eta^2\text{-}N_3]Ru(\eta^6\text{-}MeC_6H_5)$ (**1**) with excess acetylene, which generates **2** in situ. Although coordinated arene complexes may be intermediates during cyclotrimerization, the resting state of the catalyst appears to be adduct **2**; the η^6-benzene complex analogous to **1** is not observed during the catalytic reaction in THF. This is consistent with the observation that benzene solutions of **2** are not in equilibrium with significant quantities of $[\kappa^2\text{-}N_3]Ru(\eta^6\text{-}C_6H_6)$.

The cyclotrimerization reaction is catalytic, but activity is maintained only briefly, as **2** decomposes during the course of the reaction. In a typical run with 10 equiv of C_2H_2, 2.7 equiv of benzene was generated over a period of ca. 4 h (∼ 8 equiv of C_2H_2 consumed), after which catalytic activity ceases and an intractable black solid precipitates from the brown-black solution. Only benzene and residual acetylene were observed by ^{1}H NMR of the volatile components of the reaction mixture; organic products such as olefins and ene-ynes were not detected by NMR and GC-MS. The number of catalytic turnovers achieved before catalyst decomposition was not significantly affected by increasing the initial acetylene ratio from 10 to 20 equiv.

The reaction of **1** with excess propyne also leads to trimerization, generating 1,3,5-trimethylbenzene (mesitylene) as the only organic product detected by NMR and GC-MS. Approximately 1

dx.doi.org/10.1021/om100953g |*Organometallics* 2011, 30, 2125–2136

equiv of mesitylene is produced before trimerization activity ceases. An intermediate ruthenium complex can be observed by ^{1}H NMR in the reaction of **1** with 0.9 equiv of propyne and is tentatively identified as the propyne analogue of **2**, [N_3]Ru(HC≡CMe). However, this complex decomposes within minutes at room temperature, much faster than **2** during the trimerization of acetylene. Attempts to isolate the propyne adduct at low temperatures and in the absence of excess propyne were not successful. The ^{1}H NMR spectrum of [N_3]Ru(HC≡CMe) in situ indicates C_s symmetry. The imine methyl groups (δ 1.32, 1.26) and para mesityl methyls (δ 2.29, 2.26) are each inequivalent pairs, appearing as four singlets (3H each), in addition to two resonances for the meta mesityl methyls (6H each). This overall pattern of six methyl resonances (3:3:3:3:6:6) is consistent with the alkyne ligand lying in the [N_3] plane as in **2**. In contrast, the perpendicular orientation of the propyne ligand, although also of C_s symmetry, would give rise to a ^{1}H spectrum with a total of four methyl resonances (3 mesityl, 1 imine), each integrating for *six* protons (6:6:6:6). A doublet at δ 1.85 in the ^{1}H spectrum of [N_3]Ru(HC≡CMe) corresponds to the propynyl methyl group, with a measurable four-bond coupling to the propynyl proton at δ 6.78 ($^4J_{HH}$ = 2.8 Hz).

Reaction of 1 with Diphenylacetylene: Synthesis and Structure of [N_3]Ru(C_4Ph_4), 3. Treatment of the Ru(0) arene complex **1** with excess diphenylacetylene at room temperature leads to toluene loss and coupling of two alkynes to generate the metallacyclopentadienyl complex [N_3]Ru(C_4Ph_4) (**3**), isolated as a blue crystalline solid in 93% yield (eq 3).

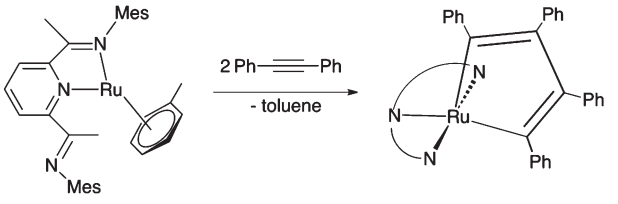

1 **3** (3)

The ^{1}H NMR spectrum of **3** is consistent with a five-coordinate, square-pyramidal geometry with an empty site trans to the apical position and indicates loss of the mirror plane coincident with the [N_3] plane. Treatment of **3** with excess phenylacetylene at temperatures up to 70 °C does not produce hexaphenylbenzene, and prolonged heating at >100 °C leads to slow decomposition.

The solid-state structure of **3** was determined crystallographically (Figure 2), revealing a distorted square-pyramidal geometry. One α-carbon of the ruthenacyclopentadienyl moiety is in the basal site, approximately trans to the pyridyl nitrogen atom (N2−Ru1−C28 172.48(8)°), and the other is apical. The ruthenacyclopentadienyl unit is approximately perpendicular to the [N_3] plane, and the Ru−C_{basal} (2.028(2) Å) and Ru−C_{apical} (2.040(2) Å) bond distances are similar and are in the range for typical Ru−C(sp^2) single bonds in ruthenoles.[9] Notably, the ruthenacyclopentadienyl C_β−C_β bond (1.465(3) Å) and C_α=C_β bonds (1.369(3), 1.368(3) Å) exhibit clear bond length alternation. The Ru−C and C−C ring distances are consistent with a 2,4-diene formulation, as opposed to the dicarbenoid metallacyclopentatriene description attributed to MC_4 systems in some instances.[10] For example, Dinjus and co-workers reported the RuC_4 ring in Cp*RuCl(2,5-Ph_2C_4) exhibits a

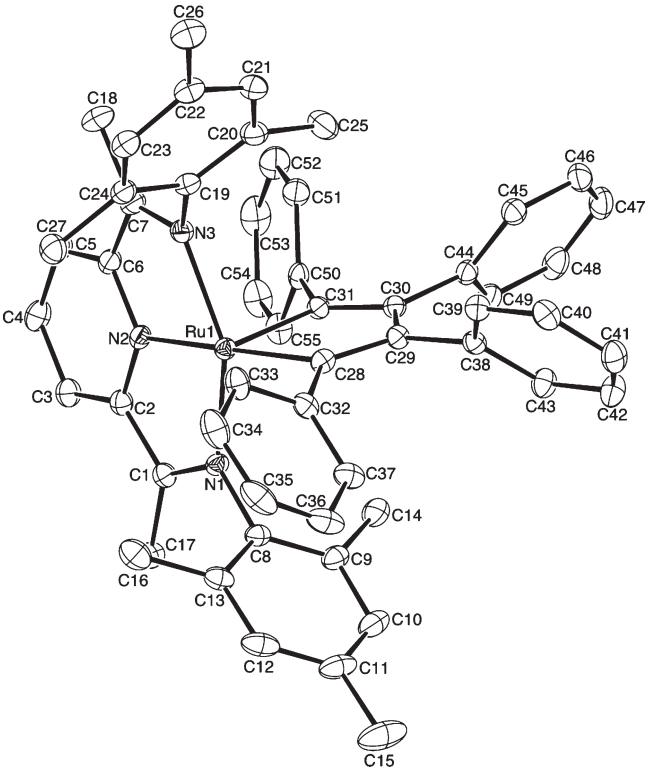

Figure 2. ORTEP drawing of [N_3]Ru(C_4Ph_4), **3**, with 30% probability thermal ellipsoids. Selected bond lengths (Å) and angles (deg): Ru1−C28, 2.028(2); Ru1−C31, 2.040(2); C28−C29, 1.368(3); C29−C30, 1.465(3), C30−C31, 1.369(3); N2−Ru1−C28, 172.48(8); N2−Ru1−C31, 94.93(8).

relatively short Ru−C (1.969(4) Å), long C_α−C_β, and short C_β=C_β bonding motif.[10b]

No intermediate with a single coordinated diphenylacetylene comparable to **2** is observed during the reaction between **1** and diphenylacetylene, prior to the formation of **3**. The diphenylacetylene analogue of **2**, with the alkyne ligand lying in the [N_3]Ru plane, is not likely due to the severe steric interactions that would result between the bulky mesityl groups on the [N_3] ligand and the alkyne. A more plausible intermediate would be the diphenylacetylene adduct with the alkyne perpendicular to the [N_3]Ru plane. Although a mono-C_2Ph_2 complex was not observed in the present case, Chirik and co-workers reported the analogous [N_3^{Ar}]Fe(C_2Ph_2) complex (Ar = 2,6-^{i}Pr$_2$C$_6$H$_3$),[11a] and a number of earlier examples of d^8 $L_3M(C_2Ph_2)$ complexes have been described as well.[11b,c] The greater bulk of the diisopropylphenyl-substituted [N_3^{Ar}] ligand employed by Chirik leads to a distorted tetrahedral geometry in the iron complex with the alkyne oriented perpendicular to the [N_3]Fe plane, compared with the square-planar coordination in **2**. Greater steric hindrance also prevents the addition of a second C_2Ph_2 molecule to form the ferrole analogous to **3**.

Metallacycle **3** is also formed in the reaction of **2** with excess diphenylacetylene (eq 4). Interestingly, unlike the reaction of **2** with CO, the C_2H_2 ligand is not displaced as free acetylene, but rather is incorporated with 2 equiv of phenylacetylene into 1,2,3,4-tetraphenylbenzene. The identity of 1,2,3,4-tetraphenylbenzene was confirmed by comparison of the

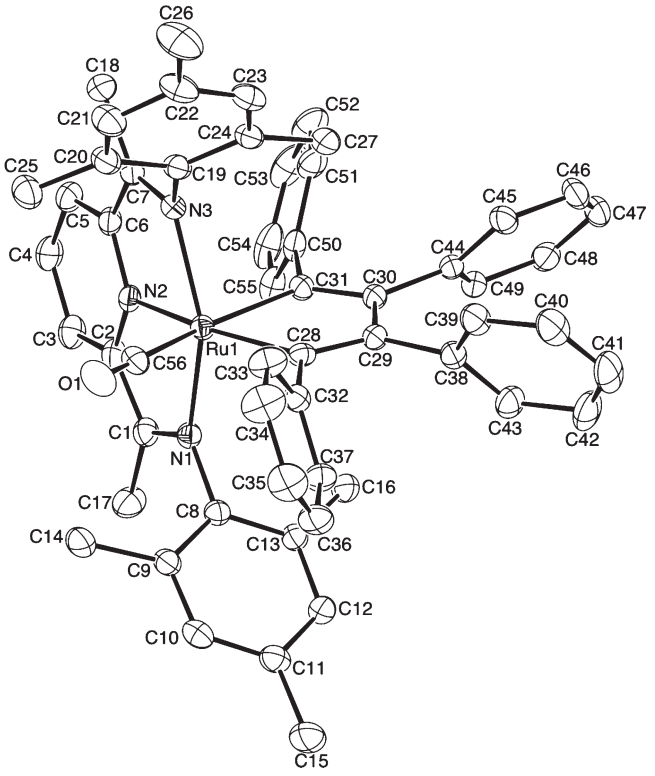

Figure 3. ORTEP drawing of $[N_3]Ru(C_4Ph_4)(CO)$, **4**, with 30% probability thermal ellipsoids. Selected bond lengths (Å): Ru1−C56, 1.910(3); Ru1−C28, 2.097(2); Ru1−C31, 2.158(2); C28−C29, 1.359(4); C29−C30, 1.481(3); C30−C31, 1.357(3); C56−O1, 1.143(3).

^{1}H NMR spectrum to the literature values[12] and GC-MS analysis.

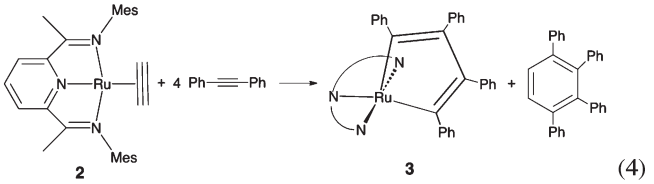

(4)

Tetraphenyl ruthenole **3** rapidly coordinates carbon monoxide to generate the orange $[N_3]Ru(C_4Ph_4)(CO)$ (**4**, 77% isolated, eq 5). The ^{1}H and ^{13}C NMR spectra of **4** are quite similar to that of the 16 e$^-$ parent compound **3**, and a band in the IR spectrum of **4** at 1926 cm^{-1} is assigned to the carbonyl ligand.

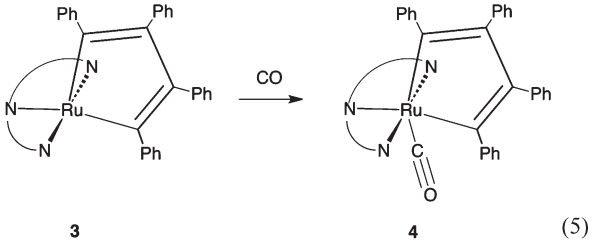

(5)

A single-crystal X-ray diffraction study confirms the structure of **4** (Figure 3). The geometry around the metal is a distorted octahedron, with the carbonyl ligand occupying the formerly vacant site of **3** and bent away from the pyridyl nitrogen atom

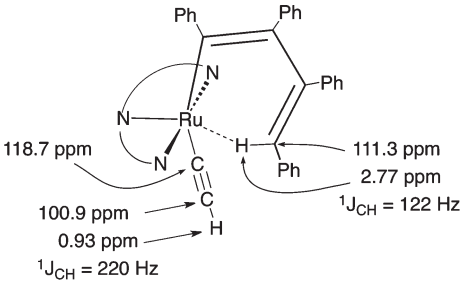

Figure 4. Selected chemical shifts and coupling constants for $[N_3]Ru(C{\equiv}C{-}H)$(*cis,cis*-1,2,3,4-tetraphenylbutadienyl-μ-H).

(107.00(10)°). Both metallacyclic Ru−C bonds are longer in **4** than **3**. The Ru−C bond trans to the carbonyl ligand in **4** (2.158(2) Å) is longer than the Ru−C bond trans to the pyridine (2.097(2) Å), reflecting the strong trans influence of the carbonyl ligand.

The ^{1}H NMR spectrum of **3** in the presence of excess trimethylphosphine at room temperature exhibits broad peaks consistent with weak and reversible coordination. The instability of the phosphine adduct is due primarily to steric congestion. Attempts to isolate the adduct were unsuccessful due to loss of PMe_3 in vacuo.

Reaction of Metallacycle 3 with Terminal Alkynes. Treatment of $[N_3]Ru(C_4Ph_4)$ (**3**) with excess acetylene at room temperature leads to addition of an acetylenic C−H bond to the ruthenium, generating a new purple complex bearing a terminal acetylide ligand and a *cis,cis*-tetraphenylbutadienyl ligand. The new C−H bond on the 4-position of the butadienyl group is agostic, interacting weakly with the metal center (eq 6).

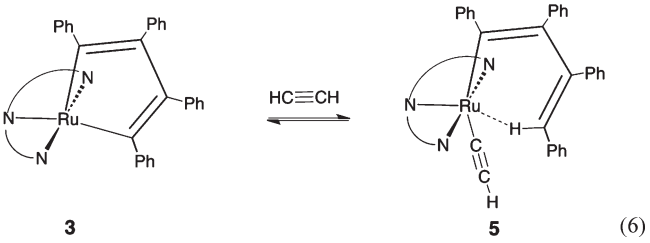

(6)

Two singlets integrating for one proton each appear in the ^{1}H NMR spectrum of **5** (δ 2.77 and 0.93). On the basis of a HMQC experiment, the peak in the ^{1}H spectrum at δ 0.93 is correlated with a ^{13}C resonance at δ 100.85 ($^1J_{CH}$ = 220 Hz). The large C−H coupling constant and chemical shift are strongly diagnostic of a proton attached to an sp-hybridized carbon atom; thus the resonance at δ 0.93 (^{1}H NMR) is assigned to the terminal acetylide proton. The proton resonance at δ 2.77 correlates with a ^{13}C signal at δ 111.3 ($^1J_{CH}$ = 122 Hz) and is assigned as the agostic proton attached to the terminal butenyl carbon (Figure 4). Assignment of the alkynyl carbon resonances was established from spectra of isotopically labeled **5**-$^{13}C_2$, generated in situ from enriched $^{13}C_2H_2$ and **3**.

The C−H coupling constant for the agostic proton is reduced compared to typical $^1J_{CH}$ values associated with an sp^2-hybridized carbon atom (148−159 Hz),[13] consistent with an agostic C−H···Ru interaction. Further evidence for the agostic C−H interaction is found in the solid-state structure (vide infra).

Surprisingly, formation of **5** from **3** and acetylene is readily reversible in solution, reverting to **3** within ca. 1 d at room

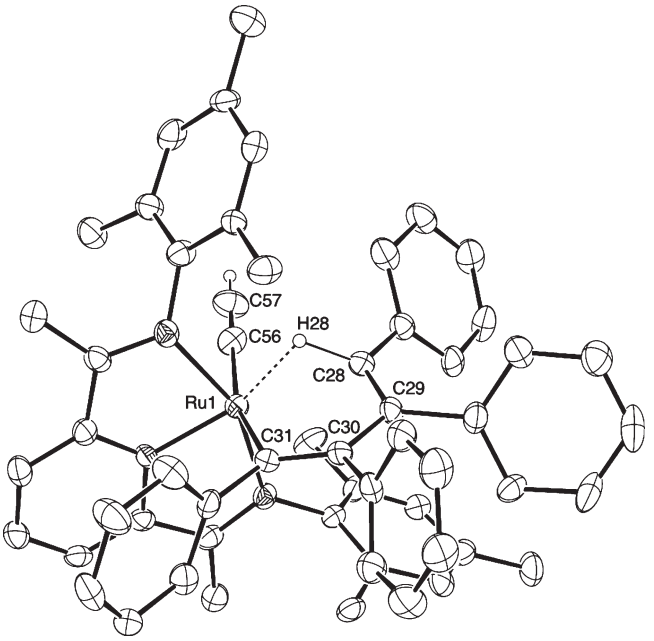

Figure 5. ORTEP drawing of $[N_3]Ru(C{\equiv}C{-}H(cis,cis\text{-}1,2,3,4\text{-tetraphenylbutadienyl-}\mu\text{-}H)$, **5**, with 30% probability thermal ellipsoids. R_1 = 14.25%. Selected distances (Å): Ru1−C28, 2.433(7).

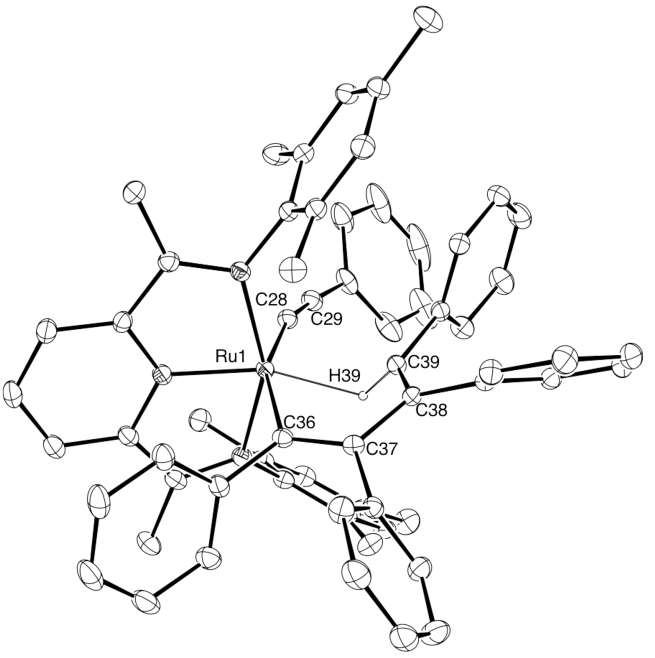

Figure 6. ORTEP drawing of $[N_3]Ru(C{\equiv}C\text{-}Ph)(cis,cis\text{-}1,2,3,4\text{-tetraphenylbutadienyl-}\mu\text{-}H)$, **6**, with 30% probability thermal ellipsoids. Selected distances (Å): Ru1−H39, 1.90(3); Ru1−C39, 2.452(2); Ru1−C36, 2.101(2), C36−C37, 1.363(3); C37−C38, 1.469(3); C38−C39, 1.369(3).

temperature in the absence of excess acetylene. The reversibility was further confirmed by treatment of **5** with ^{13}C-labeled acetylene ($^{13}C_2{}^1H_2$). Significant incorporation of the ^{13}C label into the acetylide ligand of **5** is observed within 1 h by ^{1}H and ^{13}C NMR.

Although the reversibility of the reaction prevented isolation of **5** uncontaminated with **3**, single crystals of **5** were grown from a concentrated solution under acetylene, and an X-ray structure determination was performed (Figure 5). The diffraction data collected were not of high quality, and the structure refined to a fairly high *R*-factor (R_1 = 14.25%). This is sufficient, however, to establish the overall connectivity, including the linear terminal acetylide ligand and long distance (2.433(7) Å) between Ru and terminal carbon of the *cis,cis*-butadienyl ligand. A peak was found in the difference Fourier map between the metal and terminal carbon of the C_4Ph_4 ligand, in a location consistent with the agostic C−H−Ru linkage suggested by the NMR data. Fortunately, more reliable evidence for the bridging C−H−Ru moiety is found in the structure of the phenylacetylide derivative described next.

Treatment of **3** with phenylacetylene results in a rapid reaction to generate **6** (eq 7), the phenylacetylide analogue of **5**. Formation of **6** does not appear to be readily reversible, and the compound was isolated as a dark solid in 80% yield.

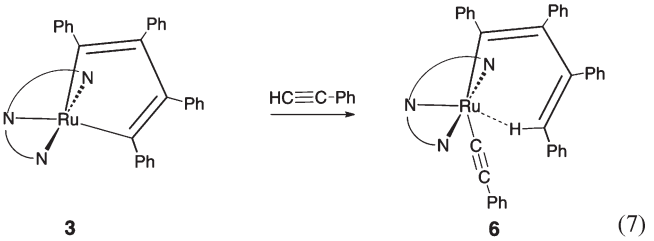

3 **6** (7)

A singlet assigned to the agostic hydride is observed at δ 3.30 in the ^{1}H NMR spectrum of **6**, which correlates to a peak in the ^{13}C NMR spectrum at δ 110.29 ($^1J_{CH}$ = 121.2 Hz) for the butenyl terminus. This relatively small C−H coupling constant is similar to that seen in **5** and is also consistent with a C−H···Ru interaction.

A single-crystal X-ray structure determination was performed for **6** (Figure 6). The geometry for **6** is distorted octahedral, with the agostic butenyl C−H coordinated trans to the pyridine. The bridging hydrogen was located and refined isotropically. Both the agostic Ru···H bond distance (1.90(3) Å) and the Ru···H−C angle (109(2)°) are well within the ranges reported for an agostic M···H−C interaction (1.8−2.3 Å, 90−140°).[14]

Synthesis and Structure of $[N_3]RuCl_2(C_2H_2)$. The acetylene dichloride $[N_3]RuCl_2(C_2H_2)$ (**7**) was prepared as a Ru(II) analogue of **2**. Generation of the known THF complex $[N_3]RuCl_2(THF)$,[15] followed by in situ treatment with acetylene, afforded **7** as a purple solid (81%) (eq 8). The acetylenic protons appear in the ^{1}H NMR spectrum of **7** at δ 5.04, which correlates to a ^{13}C NMR peak at δ 84.99.

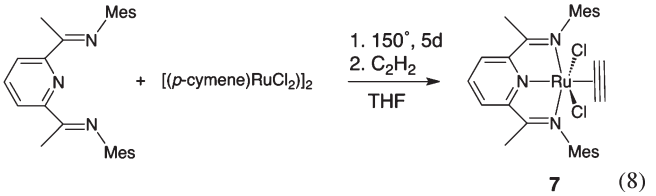

7 (8)

The solid-state structure of **7** exhibits an octahedral geometry (Figure 7), with mutually trans chlorides and the acetylene ligand lying within the $[N_3]Ru$ plane, coordinated trans to pyridine. The Ru−C bond distances (2.179(3), 2.182(4) Å) are not statistically different and are similar to the other structurally characterized ruthenium η^2-acetylene complexes reported in the

dx.doi.org/10.1021/om100953g |*Organometallics* 2011, 30, 2125–2136

literature.[7] The C≡C bond length (1.198(8) Å) is slightly elongated compared to that of free acetylene (1.181(7) Å).[6]

DFT Calculations on $[N_3]Ru(C_2H_2)$. The electronic structure of **2** was investigated computationally using the Gaussian09[16] package of programs at the B3LYP[17] level of theory employing the 6-31G(d,p) basis set[18] for C, H, and N atoms and the quasirelativistic small-core SDD pseudopotential and [6s5p3d] contracted valence basis set for Ru,[19] supplemented with two 4f-type and one 5g-type function as described by Martin and Sundermann.[20] Because of the similar chemical reactivity previously observed in $[N_3]$Ru systems containing mesityl and 2,6-xylyl groups,[3] the latter ligand was used for these studies.

The experimental solid-state and calculated geometries for **2** are shown in Figure 8, and metrical parameters listed in Table 1. Whereas the former exhibits approximately C_{2v} symmetry, the lowest energy calculated geometry has the acetylene ligand displaced slightly out of the plane of the $[N_3]$Ru core; the angle formed by the midpoint of the alkyne C−C bond, metal, and pyridine N is 170.6°. In contrast, the planar geometry optimized to a first-order saddle point with a single imaginary vibrational mode corresponding to the out-of-plane bend of the HCCH ligand (i.e., distorting toward the ground-state C_s structure). However, the energy difference between the calculated C_s ground state and C_{2v} "transition state" is negligible (ΔE_{elect} ca. 0.13 kcal mol^{-1}) and is easily within the error associated with this DFT calculation.

Interestingly, closer examination of the crystal structure reveals distinct elongation of the ruthenium and acetylenic carbon thermal ellipsoids along the axis perpendicular to the $[N_3]$Ru plane (Figure 7), suggesting either thermal motion or an unresolved crystallographic disorder. It is possible that observed anisotropy results from inversion of the nonplanar geometry as in the calculated structure, but the two required alkyne sites were too close to be refined separately at half-occupancy. In short, the calculated and experimental geometries are essentially the same within the errors of the respective methods.

As mentioned above, the $[N_3]$ ligand is potentially noninnocent, and some formally zerovalent metal complexes are more accurately described as $[N_3]^-$/M(I) or $[N_3]^{2-}$/M(II). Alkyne complex **2** is diamagnetic; thus this type of $[N_3]^-$/Ru(I) valence tautomer would correspond to a broken symmetry, open-shell singlet (i.e., antiferromagnetically coupled unpaired electrons on the metal and ligand anion). However, multiple attempts to use unrestricted DFT methods either converged to the closed-shell singlet during the SCF or yielded open-shell singlets that were found to be unstable. In contrast, the closed-shell singlet state used for the geometry optimization was confirmed to be stable[21] (i.e., exhibited no restricted−unrestricted or internal instabilities). It has been shown that the degree of noninnocence in $[N_3]$Fe complexes is most pronounced with weak field ligands

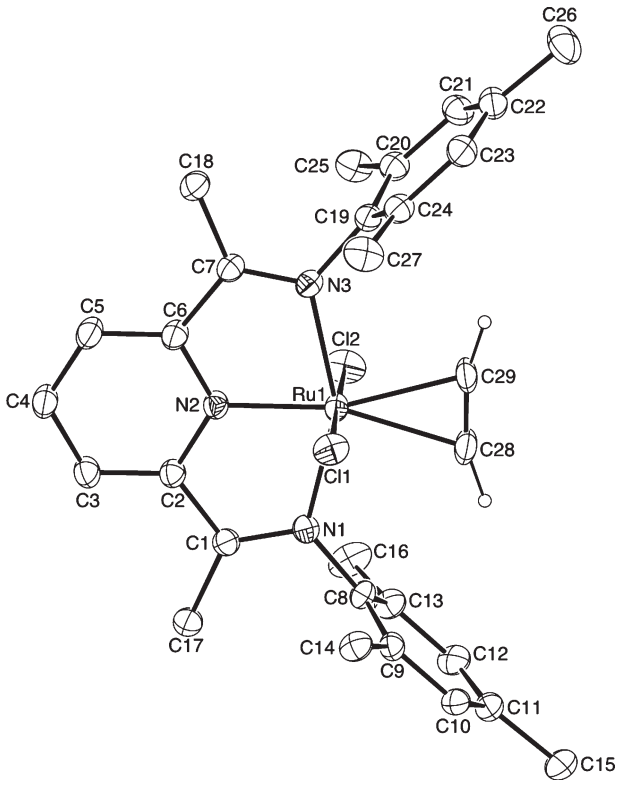

Figure 7. ORTEP drawing of $[N_3]RuCl_2(C_2H_2)$, **7**, with 30% probability thermal ellipsoids. Selected bond lengths (Å): Ru1−C29, 2.179(3), Ru1−C28, 2.182(4), C28−C29, 1.198(6).

Table 1. Comparison of Selected Experimental and Calculated Bond Distances in $[N_3]Ru(C_2H_2)$ (2)

distance (Å)	X-ray crystal structure[a]	DFT
Ru−C	2.032(2)	2.023
	2.040(2)	2.023
C≡C	1.239(4)	1.280
$Ru-N_{pyr}$	1.961(2)	1.950
$Ru-N_{im}$	2.057(2)	2.098
	2.058(2)	2.098
$C=N_{im}$	1.332(3)	1.331
	1.326(3)	1.331
$C_{ipso}-C_{im}$	1.425(3)	1.427
	1.428(3)	1.427

[a] Numbers in parentheses are estimated standard deviations in the least significant digits.

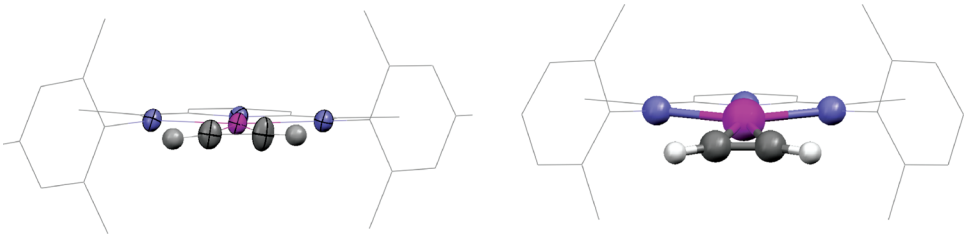

Figure 8. Comparison of experimental geometry of **2** (left) and optimized geometry from DFT calculations (right) showing ca. 10° bend of HCCH out of the $[N_3]$Ru plane.

Table 2. NMR Data for Selected η^2-Acetylene Complexes

complex	^{1}H δ (C_2H_2)	^{13}C δ (C_2H_2)
4-electron donors[a]		
$W(C_2H_2)Cl_4(Et_2O)$[b]	17.5	215.5
$W(C_2H_2)CO(S_2CNEt_2)$[c]	12.5, 13.5	206, 207
$Mo(^tBuNS)_2(^tBuNC)_2(C_2H_2)$[d]	10.43	171.7
$Mo(dppe)_2(C_2H_4)$[e]	10.18	171
$[OsH(=C=CH_2)(C_2H_2)(P^iPr_3)_2]BF_4$[f]	10.17	137.3
2-electron donors[a]		
$[Os(en)_2(C_2H_2)(C_2H_4)]^{2+}$[g]	7.3	103.4
$[Re(C_2H_2)(NO)(PPh_3)(Cp)]BF_4$[h]	6.72, 6.83	84.5, 89.7
$Ni(C_2H_2)(PPh_3)_2$[i]	6.41	122
$Re_2Cl_4(\mu\text{-dppm})_2(\mu{:}\eta^2,\eta^2\text{-}C_2H_2)(\eta^2\text{-}C_2H_2)$[j]	6.31	96.3
$Re(C_2H_2)(CO)_2(Cp)$[k]	5.61	64.5
$[Ru(C_2H_2)(PMe_2Ph)_2(Cp)]BF_4$[l]	5.57	60.4
$[Cp^*Ru(C_2H_2)(PEt_3)_2]BPh_4$[m]	4.38	66.14
$[Ru(C_2H_2)(PMe_3)_2(Cp)]BF_4$[n]	4.98	62.4

[a] Number of electrons formally donated to the metal by the acetylene ligand. [b] Ref 25d. [c] Ref 25c. [d] Ref 25a. [e] Ref 25b. [f] Ref 25e. [g] Ref.25i. [h] Ref 25k. [i] Ref 25h. [j] Ref [25h].25h [k] Ref 25g. [l] Ref 7b. [m] Ref 7a. [n] Ref 25j.

such as N_2 and *p*-dimethylaminopyridine,[5] and it is likely the acetylene in **2** is sufficiently strong field to favor the closed-shell ground state.

DISCUSSION

Bonding in [N$_3$]Ruthenium Acetylene Complexes. Bonding between the metal and the acetylene ligand in **2** and **7** can be described in part by the Dewar−Chatt−Duncanson[22] model, where the primary interaction occurs through orbitals in the M(C_2) plane (alkyne $\pi_\parallel$ to d_σ and d to alkyne $\pi_\parallel$*). In addition, the orthogonal C−C π-orbital can donate up to two electrons to a vacant metal d-orbital (alkyne $\pi_\perp$ to d). Although allowed by orbital symmetry, back-bonding from a metal d-orbital into the alkyne $\pi_\perp$* LUMO is generally insignificant due to poor overlap.

Whereas the dichloride **7** is an 18 e$^-$ ruthenium(II) complex with an unambiguous 2 e$^-$ donor alkyne ligand, the bonding in **2** warrants closer scrutiny. The 14 e$^-$ [N$_3$]Ru fragment can potentially accept 4 e$^-$ from the alkyne to achieve saturation. The molecular structures and spectroscopic properties of 2 e$^-$ and 4 e$^-$ alkyne complexes are usually diagnostic; thus comparison of **2** and **7** is instructive.

In general, metal−carbon bond distances decrease with greater electron donation from the alkyne.[23] More specifically, Carbó and co-workers have noted that Os−C distances in osmium−alkyne complexes are substantially shorter (ca. 0.15 Å) for four-electron -donor alkynes than for two-electron donors, whereas the alkyne triple-bond lengths are relatively unaffected. Significantly, the Ru−C distance in **2** is ca. 0.14 Å shorter than in **7**, although the alkyne C−C distances are similar (ca. 0.04 Å longer for **2**).

Another diagnostic for 4 e$^-$ donor ligands is the position of the alkyne resonances in the ^{1}H and ^{13}C NMR, which are generally found significantly downfield of 2 e$^-$ donors.[24] Acetylenic ^{1}H NMR shifts in structurally characterized η^2-acetylene complexes range from about δ 4.4 to 7.3 for 2 e$^-$ donors and from δ 10.2 to 13.5 for 4 e$^-$ donor complexes (Table 2),[7,25] and ^{13}C shifts range from δ 60 to 103 for 2 e$^-$ donors and δ 137 to 207 for 4 e$^-$ donors. As expected, **7** exhibits alkyne shifts (δ_H = 5.04, δ_C = 85.0) well within the 2 e$^-$ donor ranges.

Scheme 1. Mechanism for Cyclotrimerization of Acetylene

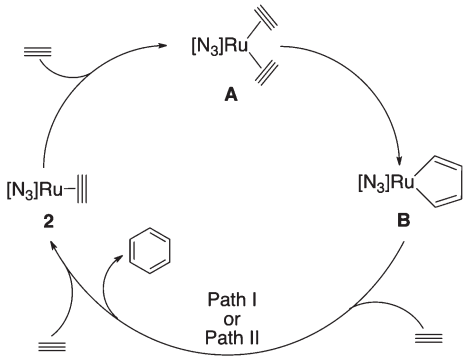

Scheme 2. [4+2] and [2+2] Mechanisms for Reaction of Metallacyclopentadienes with Acetylene

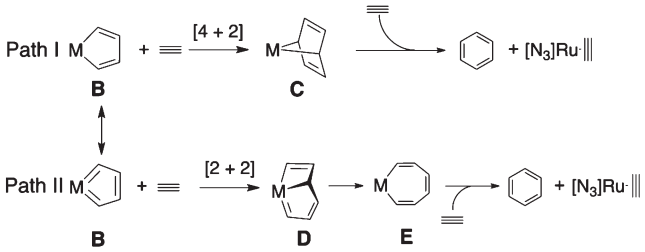

Although the short alkyne−metal distances in **2** are consistent with 4 e$^-$ donation to the metal, the NMR parameters are less conclusive. The ^{1}H resonance for the alkyne in **2** (δ_H = 6.68) is in the range expected for 2 e$^-$ donors, whereas the ^{13}C resonance (δ_C = 131.0) lies downfield of the 2 e$^-$ donor range, almost into the range observed for 4 e$^-$ donors. However, the proximity of the alkyne protons to the mesityl rings of the [N$_3$] ligand could lead to an unusually upfield shift of the ^{1}H (and ^{13}C) resonances than typically found for 4 e$^-$ donor alkynes. Overall, the chemical shift trends for **2** are consistent with a greater degree of electron donation from the acetylene to the formally Ru(0), 14 e$^-$ center than in the Ru(II) dichloride.

Mechanism of Cyclotrimerization. Metal-mediated formal [2+2+2] cyclotrimerization of alkynes has been studied extensively,[2a] and consensus has developed that metallacyclopentadienes are key intermediates in both cyclization and some cases of linear alkyne coupling.[26] Although no metallacyclic intermediates were observed during the coupling of acetylene to benzene by **2**, the formation of ruthenole **3** from PhCCPh supports the role of an analogous species in the catalytic cycle, as depicted in the mechanism proposed in Scheme 1. Reaction of **2** with a second equivalent of acetylene generates ruthenacyclopentadienyl intermediate **B**, possibly via a discrete adduct such as **A**. There are at least two precedented paths by which **B** could react with acetylene to yield benzene, and these are considered in greater detail below.

The details of the reaction between metallacycles such as **B** and a third alkyne have been a subject of considerable interest. Consistent with the bulk of previous studies, recent work by Gandon and co-workers[27] indicates that formal [4+2] cyclization between the alkyne and the metallacyclopentadiene furnishes a 7-metallanorbornadiene (**C**) (Scheme 2, path I).

dx.doi.org/10.1021/om100953g |*Organometallics* 2011, 30, 2125–2136

Reductive elimination would then give benzene. The obvious alternative mechanism—alkyne insertion into the metallacyclopentadiene to yield a seven-membered ring, followed by reductive elimination—has been considered less likely than the [4+2] addition. However, recently the groups of Schmid[28] and Yamamoto[29] have made a strong case for the intermediacy of a seven-membered metallacycle in alkyne trimerization catalyzed by certain complexes. Interestingly, these authors suggest alkyne insertion does not proceed directly, but rather involves the formal [2+2] cycloaddition of an alkyne to a M=C bond of the metallacyclopentatriene resonance structure, which is significant for some "metallacyclopentadiene" complexes. The resultant metallabicyclo[3.2.0]heptatriene intermediate (**D**) (Scheme 2, path II) rearranges to the seven-membered metallacycle (**E**), from which reductive elimination generates benzene.

Scheme 3. Comparison of Reactivity of 3 with Diphenylacetylene or Terminal Alkynes versus the Reactivity of 2 with Diphenylacetylene

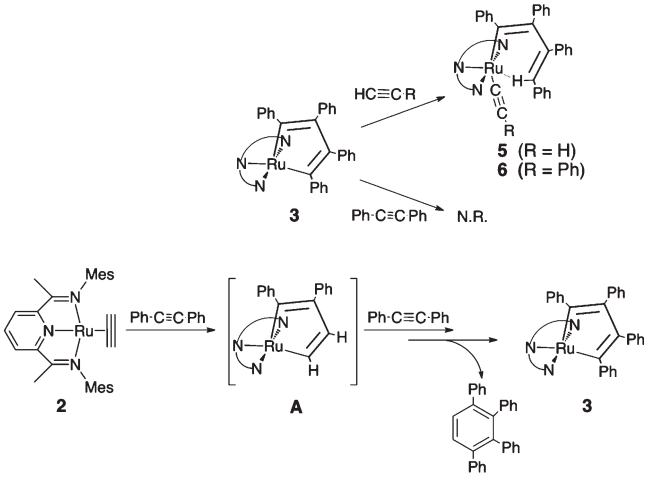

The geometric parameters for ruthenole **3** clearly suggest the ruthenacyclopentadiene depiction is preferred over ruthenacyclopentatriene, and this would seem to favor path I over path II. Note, however, that **3** does not react with alkynes to yield trimerization products and that path II cannot be ruled out in the trimerization of parent acetylene or in the reaction of **2** with diphenylacetylene to give tetraphenylbenzene. In either case, steric bulk of the metallacycle—combined with the bulky mesityl groups on the [N_3] ligand—would likely hinder access to the MC_4 π system by an incoming alkyne. The observation that **3** does not participate in alkyne cyclization reactions is consistent with steric inaccessibility of the ruthenacyclic π system.

Comparing the reactivity of **3** with diphenylacetylene or terminal alkynes versus the reactivity of **2** with diphenylacetylene further illustrates the role of ruthenacycle sterics in cyclization (Scheme 3). The steric bulk of **3** prevents cyclization with diphenylacetylene, although the less hindered end-on approach of the C−H bond of terminal alkynes permits formation of agostic complexes **5** and **6**. In contrast, coupling of diphenylacetylene and acetylene can be accomplished if the sequence of alkyne addition is reversed: C_2H_2 complex **2** reacts with excess diphenylacetylene to yield tetraphenylbenzene. The intermediate ruthenacycle for this cyclization

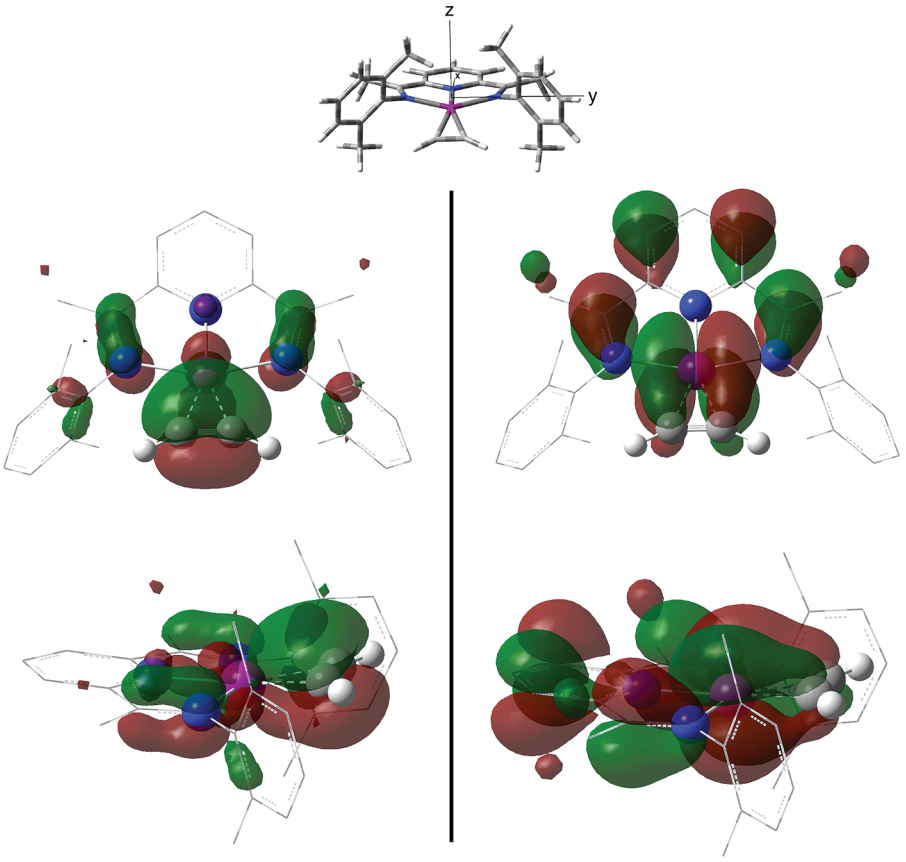

Figure 9. Molecular orbitals involving the acetylene π-orbitals perpendicular to the [N_3]Ru plane in **2**: Acetylene $\pi_\perp$ to Ru d_{xz} donation (left, HOMO−11) and weak Ru d_{yz} to $\pi_\perp^*$ back-donation (right, HOMO−2). Top and bottom figures are of each MO viewed from different perspectives.

dx.doi.org/10.1021/om100953g |*Organometallics* 2011, 30, 2125–2136

(**A**, Scheme 3), although not observed, would be diphenyl- rather than tetraphenyl-substituted and thus less hindered than **3**, and apparently permits reaction with a second equivalent of PhCCPh.

The agostic complexes **5** and **6** suggest at least one explanation for the short lifetime of **2** under catalytic conditions. In analogy with the formation of **5**, a secondary path for reaction of acetylene with the parent metallacyclopentadiene by addition of the acetylenic C−H bond would produce the acyclic butadienyl species, possibly stabilized by an agostic C−H interaction. Subsequent insertion(s) of acetylene into either the acetylide or butadienyl Ru−C bonds could lead to a distribution of polyene oligomers that could be difficult to characterize and might retain the ruthenium complex.

CONCLUSIONS

The reaction of $[\kappa^2\text{-}N_3]Ru(\eta^6\text{-}MeC_6H_5)$ (**1**) with acetylene generates the formally Ru(0) acetylene complex $[N_3]Ru(C_2H_2)$ (**2**). Spectroscopic, structural, and computational evidence suggest significant participation of the acetylene π-orbitals orthogonal to the RuC_2 plane ($\pi_\perp$), which is consistent with the 14 e^- count of the parent $[N_3]Ru$ fragment. However, the NMR data suggest $\pi_\perp$ donation is weaker in **2** than in many 4 e^- donor alkyne complexes. DFT calculations also indicate **2** is appropriately described by a closed-shell singlet wave function and that **2** is adequately described by the Ru(0) formal oxidation state.

The behavior of $[N_3]Ru(C_2H_2)$ (**2**) as an alkyne cyclotrimerization catalyst and the lack of trimerization activity for $[N_3]Ru(C_4Ph_4)$ (**3**) both shed light on the trimerization mechanism. In particular, the sterics of the intermediate metallacycle plays a key role in determining the outcome of the reaction. For example, the isolated ruthenole **3** is a model for a likely intermediate. However, trimerization requires the interaction of an alkyne with the metallacyclic π system, and this is prevented by the steric bulk of the MC_4 moiety. In contrast, acetylene complex **2** reacts with either acetylene or diphenylacetylene to generate trimerization products. In these cases, the likely—although unobserved—intermediate ruthenoles are less bulky and allow access of a third alkyne.

EXPERIMENTAL SECTION

General Methods. All manipulations were performed in Schlenk-type glassware on a dual-manifold Schlenk line or in a nitrogen-filled Vacuum Atmospheres glovebox.[30] All glassware was oven-dried prior to use. Infrared spectra were recorded on a Perkin-Elmer Spectrum 100 FT-IR spectrometer. GC-MS analyses were performed with an Agilent 6890 GC system coupled to an Agilent 5973 mass-selective detector. NMR spectra were obtained at 300, 360, and 500 MHz on Bruker DMX-300, AM-360, and AMX-500 FT NMR spectrometers, respectively. $^{13}C\{^1H\}$ NMR spectra were recorded with broadband ^1H decoupling on a Bruker DMX-360 spectrometer, and proton-coupled ^{13}C spectra were recorded using a gated decoupling sequence. All NMR spectra were recorded at 300 K unless stated otherwise. Chemical shifts are reported relative to tetramethylsilane for ^1H and ^{13}C spectra. The temperature of the NMR probe for all variable-temperature studies was calibrated against methanol.

Materials. Hydrocarbon solvents were dried over Na/K alloy-benzophenone. Benzene-d_6, toluene-d_8, and tetrahydrofuran-d_8 were dried over Na/K alloy. Chloroform-*d* was dried over activated 4 Å molecular sieves. Acetylene (Airco) was purified according to literature procedures.[31] Acetylene-$^{13}C_2$ (Cambridge Isotope Laboratories) was degassed prior to use. Ethylene and CO (Airco) were used as received. Trimethylphosphine was prepared according to literature procedures.[32] Propyne (Aldrich) was degassed prior to use. Triethylsilane (Aldrich) was dried over Na prior to use. Ruthenium complex $[\kappa^2\text{-}N_3]Ru(\eta^6\text{-}MeC_6H_5)$ (**1**) was synthesized according to the literature procedure.[3] Abbreviations used: Mes = 1,3,5-trimethylphenyl; $[N_3]$ = 2,6-(MesN=CMe)$_2C_5H_3N$.

DFT Calculations. All calculations were performed using the Gaussian09[16] package of programs at the B3LYP[17] level of theory employing the 6-31G(d,p) basis set[18] for C, H, and N atoms and the quasirelativistic small-core SDD pseudopotential and [6s5p3d] contracted valence basis set[19] for Ru, supplemented with two 4f-type and one 5g-type function as described by Martin and Sundermann.[20] Calculated energy minima for optimized geometries were confirmed as a stationary point by the absence of imaginary vibrational modes in a subsequent frequency calculation. All wave functions derived from single-point energy calculations were confirmed to exhibit no restricted−unrestricted or internal instabilities.[21]

Synthesis of $[N_3]Ru(C_2H_2)$, 2. A round-bottomed flask was charged with $[\kappa^2\text{-}N_3]Ru(\eta^6\text{-}MeC_6H_5)$ (**1**) (200 mg, 0.339 mol), and diethyl ether (ca. 15 mL) was vacuum transferred into the reaction vessel. The solution was cooled to −196 °C, and acetylene (0.44 mmol, 1.3 equiv) was measured out with a calibrated gas bulb and condensed into the vessel. The reaction mixture was warmed to room temperature and stirred 10 min, upon which the color of the solution turned green. Recrystallization from diethyl ether afforded 112 mg (63% yield) of **2** as green crystals. ^1H NMR (C_6D_6; δ): 7.92 (d, 2H, Py-H_m), 7.81 (t, 1H, Py-H_p), 6.91 (s, 4H, Mes-H_m), 6.68 (s, 2H, C_2H_2), 2.26 (s, 6H, Mes-Me_p), 1.99 (s, 12H, Mes-Me_o), 1.28 (s, 6H, Im-*Me*). ^1H NMR (THF-d_8; δ): 8.26 (d, 2H, $^3J_{HH}$ = 7.7 Hz, Py-H_m), 7.98 (t, 1H, $^3J_{HH}$ = 7.7 Hz, Py-H_p), 7.05 (s, 4H, Mes-H_m), 6.10 (s, 2H, Ru(C_2H_2), 2.41 (s, 6H, Mes-Me_p), 1.87 (s, 12H, Mes-Me_o), 1.51 (s, 6H, Im-*Me*). $^{13}C\{^1H\}$ NMR (THF-d_8; δ): 153.86, 153.81, 145.90, 135.11, 130.91 (quaternary), 131.00 ($^1J_{CH}$ = 226.4 Hz, C_2H_2), 129.25 (Mes-C_m), 118.60 (Py-C_m), 117.34 (Py-C_p), 21.30, 19.36, 18.53 (Mes-Me_p and Im-*Me*).

Reaction of $[\kappa^2\text{-}N_3]Ru(\eta^6\text{-}MeC_6H_5)$ (1) with CO. An NMR tube equipped with a PTFE needle valve was loaded with a benzene-d_6 solution (0.3 mL) of **1** (5 mg, 0.0095 mmol). The solution was degassed, and 1 atm of CO was backfilled into the NMR tube. Only $[N_3]Ru(CO)_2$ and free acetylene were observed by ^1H NMR. ^1H NMR of $[N_3]Ru(CO)_2$ (C_6D_6; δ): 7.11 (d, 2H, Py-H_m), 6.93 (t, 1H, Py-H_p), 6.80 (s, 4H, Mes-H_m), 2.13 (s, 6H, Mes-Me_p or Im-*Me*), 2.11 (s, 6H, Mes-Me_p or Im-*Me*), 2.02 (s, 12H, Mes-Me_o).

Reaction of $[N_3]Ru(C_2H_2)$ (2) with Excess Acetylene. An NMR tube equipped with a PTFE needle valve was loaded with a cyclohexane-d_{12} solution (0.3 mL) of **2** (2 mg, 0.00381 mmol) with 1 μL of hexamethyldisiloxane added as an internal integration standard. The solution was degassed, and excess acetylene (0.04 mmol, ca. 10.5 equiv) was measured out with a calibrated gas bulb and condensed into the NMR tube. The reaction was monitored by ^1H NMR until all **2** was consumed, at which time the reaction mixture contained 2.7 equiv of benzene compared to **2** originally present.

Reaction of $[\kappa^2\text{-}N_3]Ru(\eta^6\text{-}MeC_6H_5)$ (1) with Propyne. An NMR tube equipped with a PTFE needle valve was loaded with a C_6D_6 solution (0.3 mL) of **1** (10 mg, 0.0169 mmol). The solution was degassed, and a slight deficit of propyne (0.015 mmol, ca. 0.9 equiv) was measured out with a calibrated gas bulb and condensed into the NMR tube. Following thawing, the solution was monitored by ^1H NMR and was found to contain ca. 10% 1,3,5-trimethylbenzene (mesitylene) and an unstable complex tentatively assigned as $[N_3]Ru(HC{\equiv}CMe)$. ^1H NMR of mesitylene (C_6D_6; δ): 6.71 (s, 3H, Ar-*H*), 2.15 (s, 9H, Ar-*Me*). ^1H NMR of $[N_3]Ru(HC{\equiv}CMe)$ (C_6D_6; δ): 8.01 (d, 1H, Py-H_m), 7.97 (d, 1H, Py-H_m), 7.80 (t, 1H, Py-H_p), 6.93 (s, 2H, Mes-H_m), 6.91 (s, 2H, Mes-H_m), 6.78 (br, 1H, *HC*≡C), 2.29, 2.26 (both s, 3H, Mes-Me_p), 2.02, 1.98 (both s, 6H, Mes-Me_o), 1.85 (d, 3H, $^4J_{HH}$ = 2.8 Hz, −C≡*CMe*), 1.32, 1.26 (both s, 3H, Im-*Me*).

Synthesis of [N$_3$]Ru(C$_4$Ph$_4$), 3. A round-bottomed flask was charged with [η^2-N$_3$]Ru(η^6-MeC$_6$H$_5$) (**1**) (150 mg, 0.254 mmol) and diphenylacetylene (100 mg, 0.561 mmol, 2.2 equiv). The reactants were dissolved in toluene (4 mL) and stirred for 1 h, whereupon the solution turned bright blue. Recrystallization from toluene yielded 200 mg of **3** as a crystalline blue solid (92% yield). ^{1}H NMR (C$_6$D$_6$; δ): 7.29 (d, 2H, aryl-*H*), 7.13−6.98 (m, aryl-*H*), 6.94 (t, aryl-*H*), 6.87−6.69 (m, 6H, aryl-*H*), 6.46 (s, 2H, Mes-*H*$_m$), 6.40 (t, 2H), 5.64 (d, 2H), 5.70 (d, 2H), 2.72, 2.10, 1.48, 1.13 (all s, 6H, Im-*Me* and Mes-*Me*). ^{1}H NMR (THF-*d*$_8$; δ): 7.68 (d, 2H, Py-*H*$_m$), 7.44 (t, 1H, Py-*H*$_p$), 6.93 (s, 2H, Mes-*H*$_m$), 6.78 (s, 2H, Mes-*H*$_m$), 6.57−6.48 (m, aryl-*H*), 6.38 (t, 2H, aryl-*H*), 6.30 (t, 2H, aryl-*H*), 5.46 (d, 2H, aryl-*H*), 5.20 (d, 2H, aryl-*H*), 2.51, 2.25, 1.85, 1.12 (all s, 6H, Im-*Me* and Mes-*Me*). ^{13}C{^{1}H} NMR (THF-*d*$_8$; δ): 215.76, 169.24, 158.48, 156.26, 153.44, 151.00, 147.45, 144.61, 144.18, 141.49, 140.88, 135.26 (all quaternary), 133.43 (aryl-CH), 132.43 (quaternary), 131.98 (aryl-CH), 130.07 (quaternary), 129.84, 129.76, 129.27, 129.07, 127.84, 127.73, 126.95, 126.79, 126.73, 126.95, 126.79, 126.72, 126.21, 123.96, 123.26, 122.17, 121.18 (all aryl-CH), 21.08, 20.16, 17.96, 17.84 (Im-*Me* and Mes-*Me*).

Reaction of [N$_3$]Ru(C$_2$H$_2$) (2) with Diphenylacetylene. An NMR tube was loaded with a benzene-*d*$_6$ solution (0.4 mL) of [N$_3$]Ru(C$_2$H$_2$) (**2**) (5 mg, 0.0095 mmol) and diphenylacetylene (7 mg, 4.2 equiv). The NMR tube was flame-sealed, and the reaction was monitored by ^{1}H NMR. All of the [N$_3$]Ru(C$_2$H$_2$) (**2**) initially present was consumed within 1.5 h, and both **3** and 1,2,3,4-tetraphenylbenzene were observed by ^{1}H NMR. The reaction mixture was eluted through a silica gel column to separate the 1,2,3,4-tetraphenylbenzene. ^{1}H NMR of tetraphenylbenzene (CDCl$_3$; δ): 7.50 (s, 2H), 7.12 (m, 10H), 6.92 (m, 10H), 6.80 (m, 4H). MS (CI): calcd 383.1704 [M + H]$^+$, found 383, calcd 411.2107 [M + C$_2$H$_5$]$^+$ 411

Synthesis of [N$_3$]Ru(C$_4$Ph$_4$)(CO), 4. A 10 mL round-bottomed flask was charged with **3** (30 mg, 0.035 mmol), and toluene (4 mL) was vacuum transferred into the reaction vessel. CO (200 Torr) was admitted, and the resultant slurry was stirred for 0.5 h. The reaction mixture was filtered and dried in vacuo to afford 24 mg of **4** as an orange solid (77% yield). ^{1}H NMR (C$_6$D$_6$; δ): 7.20 (d, 2H), 7.08−6.89 (m), 7.72−6.88 (m), 6.48 (t, 2H), 6.07 (d, 2H), 5.92 (d, 2H), 2.99, 2.18, 1.72, 1.66 (all s, 6H, Im-*Me* and Mes-*Me*). ^{1}H NMR (THF-*d*$_8$; δ): 7.61 (d, 2H, Py-*H*$_m$), 7.51 (t, 1H, Py-*H*$_p$), 7.00 (s, 2H, Mes-*H*$_m$), 6.81 (s, 2H, Mes-*H*$_m$), 6.63−6.45 (m), 6.36 (d), 5.97 (d, 2H, Ar-*H*), 5.42 (d, 2H, Ar-*H*), 2.79, 2.33, 2.28, 1.72 (all s, 6H, Im-*Me* and Mes-*Me*). ^{13}C{^{1}H} NMR (THF-*d*$_8$; δ): 194.06, 191.58, 184.49, 170.87, 158.98, 154.87, 154.06, 150.34, 147.68, 145.98, 145.29, 136.13, 132.67 (all quaternary), 132.20, 130.87, 130.46, 129.83, 129.74, (all Ar-CH), 128.82 (quaternary), 127.40, 127.04, 126.80, 126.57, 126.50, 125.33, 123.63, 123.06, 121.93, 121.41 (all Ar-CH), 21.12, 21.02, 18.59, 17.77 (Im-*Me* and Mes-*Me*). Ir (Nujol): ν(CO) 1926 cm^{-1}. HRMS (ES): calcd 883.3076 (M(^{102}Ru))$^+$, found 883.3103.

Observation of [N$_3$]Ru(C≡C-H)(*cis*,*cis*-1,2,3,4-tetraphenylbutadienyl-μ-H), 5. An NMR tube equipped with a PTFE needle valve was loaded with a THF-*d*$_8$ solution (0.3 mL) of [N$_3$]Ru(C$_4$Ph$_4$) (**3**) (10 mg, 0.012 mmol). Excess acetylene (0.06 mmol, 5 equiv) was measured out with a calibrated gas bulb and condensed into the NMR tube. Following thawing, the solution changes from blue to purple over a period of 5 min. Attempts to isolate pure **5** were thwarted by reversion to **3** in vacuo. A small number of crystals of **5** were fortuitously grown under excess acetylene and used for the X-ray study. ^{1}H NMR (THF-*d*$_8$; δ): 7.69 (d, 2H, $^3J_{HH}$ = 7.9 Hz, Py-*H*$_m$), 7.35 (d, 1H, $^3J_{HH}$ = 7.9 Hz, Py-*H*$_p$), 7.16 (m, 2H, Ar-*H*), 6.91 (s, 2H (Mes-*H*$_m$), 6.85 (m, 2H, Ar-*H*), 6.76 (m, 2H, Ar-*H*), 6.68 (s, 2H, Mes-*H*$_m$), 6.57−6.41 (m, 10H, Ar-*H*), 5.94 (d, J_{HH} = 7.4 Hz, Ar-*H*), 5.74 (d, J_{HH} = 7.4 Hz, Ar-*H*), 2.77 (s, 1H, Ru···*H*C), 2.51, 2.32, 2.25, 1.87 (all s, 6H, Im-*Me* and Mes-*Me*), 0.93 (s, 1H, Ru-CC*H*). ^{13}C NMR (THF-*d*$_8$; δ): 212.38, 167.29, 167.37, 156.00, 148.95, 148.91, 148.07, 143.22, 143.05, 140.97, 135.59, 134.48 (all quaternary), 133.44, 132.58, 131.45 (all Ar-*C*H), 131.31 (quaternary), 130.41, 129.96, 129.85, 129.08, 127.32, 127.03, 126.96, 126.52, 126.22, 126.10, 125.01, 124.92, 124.27, 124,05, 122.36, 121.64 (all Ar-CH), 118.77 ($^1J_{CC}$ = 106.2 Hz, Ru-*C*C), 111.13 ($^1J_{CH}$ = 122 Hz, Ru···H-*C*), 100.85 ($^1J_{CC}$ = 106.2 Hz, $^1J_{CH}$ = 220 Hz, Ru-C*C*-H), 22.44, 21.02, 20.89, 17.56 (Im-*Me* and Mes-*Me*).

Reversibility of Formation of 5: Reaction of 5 with ^{13}C$_2$H$_2$. An NMR tube equipped with a PTFE needle valve was loaded with a THF-*d*$_8$ (0.3 mL) solution of [N$_3$]Ru(C$_4$Ph$_4$) (**3**) (6 mg, 0.007 mmol), and excess acetylene (0.01 mmol, 1.4 equiv) was condensed into the tube. The reaction was monitored by ^{1}H NMR until formation of **5** was complete, whereupon excess acetylene-$^{13}C_2$ (0.014 mmol, 2 equiv) was condensed into the NMR tube. The reaction was monitored by ^{1}H and ^{13}C NMR. Incorporation of the ^{13}C label into **5** was observed within 0.5 h. ^{13}C NMR (THF-*d*$_8$; δ): 118.77 ($^1J_{CC}$ = 106.1 Hz, Ru-*C*C 111.13 ($^1J_{CH}$ = 122 Hz, $^1J_{CC}$ = 106.1 Hz, Ru···H-*C*).

Synthesis of [N$_3$]Ru(C≡C-Ph)(*cis*,*cis*-1,2,3,4-tetraphenylbutadienyl-μ-H), 6. A round-bottomed flask was charged with **4** (150 mg, 0.0175 mmol), and toluene was added (5 mL). A slight excess of phenylacetylene (23 μL, 0.0209 mmol, 1.2 equiv) was added, effecting an immediate color change from blue to brown. Recrystallization from toluene afforded 135 mg of **6** (80% yield) as a brown solid. ^{1}H NMR (C$_6$D$_6$; δ): 7.22 (d, 2H, Ar-*H*), 7.05 (t, 2H, Ar-*H*), 6.98−6.95 (m, Ar-*H*), 6.91−6.89 (m, Ar-*H*), 6.85−6.71 (m, Ar-*H*), 6.63 (m, 2H, Ar-*H*), 6.50 (t, 2H, Ar-*H*), 6.38 (d, 2H, Ar-*H*), 5.94 (d, 2H, Ar-*H*), 3.30 (s, 1H, Ru···*H*C), 2.70, 2.15, 2.14, 1.92 (all s, 6H, Im-*Me* and Mes-*Me*). ^{1}H NMR (CDCl$_3$; δ): 7.49 (d, 2H, Py-*H*$_m$), 7.26 (t, 1H, Py-*H*$_o$), 6.88 (m, Ar-*H*), 6.74 (s, 2H, Mes-*H*$_m$), 6.68−6.49 (m, Ar-*H*), 6.39 (t, 2H, Ar-*H*), 5.87 (d, 2H, Ar-*H*), 5.75 (d, 2H, Ar-*H*), 2.83 (s, 1H, Ru···*H*), 2.55, 2.34, 2.30, 1.94 (all s, 6H, Im-*Me* and Mes-*Me*). ^{13}C NMR (CDCl$_3$ δ): 166.24, 164.67, 154.97, 147.84, 142.15, 142. 06, 141.47, 141.31, 139.80, 135.14, 133.27 (all quaternary), 131.98, 131.60, 131.10, 130.57 (all Ar-CH), 130.57 (quaternary), 129.77, 129.38, 127.12, 126.73, 126.43, 126.01, 125.62, 124.13, 123.95, 123.79, 123.75, 123.63, 123.59, 122.89, 121.73, (all Ar-CH), 120.87 (quaternary), 110.29 ($^1J_{CH}$ = 121.2 Hz, Ru···H-C), 20.98, 20.64, 20.36, 17.59 (Im-*Me* and Mes-*Me*).

Synthesis of [N$_3$]RuCl$_2$(C$_2$H$_2$), 7. A thick-walled, tubular reaction vessel was charged with 200 mg (0.0503 mmol) of the [N$_3$] ligand, 2,6-(MesN=CMe)$_2$C$_5$H$_3$N, and 154 mg of [(*p*-cymene)RuCl$_2$]$_2$ (0.0252 mmol). THF (15 mL) was vacuum transferred into the reaction vessel, which was then heated in a 150 °C oil bath until all of the reactants were consumed (5 d), as evidenced by ^{1}H NMR. The resultant solution was transferred into a swivel frit assembly, and the volume of THF was reduced to ca. 5 mL. Excess acetylene (2.5 mmol, ca. 5 equiv) was measured out with a calibrated gas bulb and condensed into the reaction vessel, and the mixture was stirred for 1 h at room temperature. Recrystallization from THF under an acetylene atmosphere afforded 243 mg of **7** as a crystalline, purple solid (81%). ^{1}H NMR (C$_6$D$_6$; δ): 7.01 (d, 2H, Py-*H*$_m$), 6.77 (t, 1H, Py-*H*$_p$), 6.68 (s, 4H, Mes-*H*$_m$), 5.44 (s, 2H, C$_2$*H*$_2$), 2.39 (s, 12H, Mes-*Me*$_o$), 2.08, 2.05 (s, 6H, Mes-*Me*$_p$ and Im-*Me*). ^{1}H NMR (CDCl$_3$; δ): 8.05 (d, 2H, Py-*H*$_m$), 7.79 (t, 1H, Py-*H*$_p$), 6.92 (s, 4H, Mes-*H*$_m$), 5.04 (s, 2H, Ru(C$_2$H$_2$), 2.73, 2.31 (s, 6H, Mes-*Me*$_p$ and Im-*Me*) 2.15 (s, 12H, Mes-*Me*$_o$). ^{13}C{^{1}H} NMR (CDCl$_3$; δ): 174.62, 157.02, 145.33, 136.36, 131.28 (all quaternary), 129.88 (Mes-*C*$_m$), 118.60 (Py-*C*$_p$), 117.34 (Py-*C*$_m$), 84.99 (*C*$_2$H$_2$), 19.36 (Mes-*Me*$_o$), 20.91, 18.93 (Mes-*Me*$_p$ and Im-*Me*).

Single-Crystal X-ray Diffraction Analysis: General Procedures. X-ray intensity data were collected on a Rigaku Mercury CCD area detector employing graphite-monochromated Mo Kα radiation (λ = 0.71069 Å) at a temperature of 143 K. Preliminary indexing was performed from a series of 12 0.5° rotation images with exposures of 30 s. Oscillation images were processed using CrystalClear,[33] producing a listing of unaveraged F^2 and $\sigma(F^2)$ values, which were then passed to the CrystalStructure[34] program package for further processing and structure

solution. The intensity data were corrected for Lorentz and polarization effects and for absorption using REQAB. The structures were solved by direct methods (SIR97).[35] Refinement was by full-matrix least-squares based on F^2 using SHELXL-97.[36] All reflections were used during refinement (F^2's that were experimentally negative were replaced by $F^2 = 0$). Non-hydrogen atoms were refined anisotropically, and hydrogen atoms were refined using a "riding" model, except hydride hydrogen atoms, which were refined isotropically, unless otherwise noted.

[N_3]Ru(C_2H_2) (2). Suitable X-ray quality crystals of **2** were grown by slow evaporation of a diethyl ether solution.

[N_3]Ru(C_4Ph_4) (3). Suitable X-ray quality crystals of **3** were grown by slow diffusion of cyclohexane into a concentrated toluene solution.

[N_3]Ru(C_4Ph_4)(CO) (4). Suitable X-ray quality crystals of **4** were grown by slow evaporation of a cyclohexane solution. There were two areas of disordered solvent (cyclohexane). The X-ray data were corrected for the presence of disordered solvent using SQUEEZE.[37]

[N_3]Ru(C≡C-H)(*cis*,*cis*-1,2,3,4-tetraphenylbutadienyl-μ-H) (5). Marginal quality crystals of **5** were grown by slow evaporation of a diethyl ether solution under an acetylene atmosphere. Non-hydrogen atoms were refined anisotropically, and hydrogen atoms were refined using a "riding" model, except H28 (the agostic Ru−H−C), which was not refined but was included as a constant contribution to the structure factors. The diffraction data collected were not of high quality, and the structure refined to a fairly high *R*-factor (R_1 = 14.25%), but is sufficient to establish the general connectivity.

[N_3]Ru(C≡C-Ph)(*cis*,*cis*-1,2,3,4-tetraphenylbutadienyl-μ-H) (6). Suitable X-ray quality crystals of **6** were grown by slow evaporation of a diethyl ether solution. Non-hydrogen atoms were refined anisotropically, and hydrogen atoms were refined using a "riding" model, except H39 (the agostic Ru−H−C), which was refined isotropically.

[N_3]RuCl_2(C_2H_2) (7). Suitable X-ray quality crystals of **7** were grown by slow evaporation of a diethyl ether solution.

■ ASSOCIATED CONTENT

Supporting Information. X-ray crystallographic data (in CIF format) and ^{1}H NMR spectra of purified samples are available free of charge via the Internet at http://pubs.acs.org.

■ AUTHOR INFORMATION

Corresponding Author

*E-mail: berry@sas.upenn.edu.

■ ACKNOWLEDGMENT

We are grateful to the National Science Foundation for support of this work under grants CHE-9904798 and CHE-0131132.

■ REFERENCES

(1) (a) Collman, J. P.; Hegedus, L. S.; Norton, J. R.; Fink, R. G. *Principles and Application of Organotransition Metal Chemistry*; University Science Books: Mill Valley, CA, 1987 (b) Agenet, N.; Buisine, O.; Slowinski, F.; Gandon, V.; Aubert, C.; Malacria, M. *Organic Reactions*; John Wiley & Sons: New York, 2007; Vol. 68.

(2) (a) Saito, S.; Yamamoto, Y. *Chem. Rev.* **2000**, *100*, 2901–2915. (b) Lautens, M.; Klute, W.; Tam, W. *Chem. Rev.* **1996**, *96*, 49–92. (c) Ojima, I.; Tzamarioudaki, M.; Li, Z.; Donovan, R. *Chem. Rev.* **1996**, *96*, 635–662.

(3) Gallagher, M.; Wieder, N. L.; Dioumaev, V. K.; Carroll, P. J.; Berry, D. H. *Organometallics* **2010**, *29*, 591–603.

(4) Wieder, N. L.; Gallagher, M.; Carroll, P. J.; Berry, D. H. *J. Am. Chem. Soc.* **2010**, *132*, 4107–4109.

(5) (a) Bart, S. C.; Chlopek, K.; Bill, E.; Bouwkamp, M. W.; Lobkovsky, E.; Neese, F.; Wieghardt, K.; Chirik, P. J. *J. Am. Chem. Soc.* **2006**, *128*, 13901–13912. (b) Bart, S. C.; Lobkovsky, E.; Bill, E.; Wieghardt, K.; Chirik, P. J. *Inorg. Chem.* **2007**, *46*, 7055–7063.

(6) Allen, F. H.; Kennard, O.; Watson, D. G.; Brammer, L.; Orpen, A. G. *J. Chem. Soc., Perkin Trans. 2* **1987**, S1.

(7) (a) Bustelo, E.; Carbo, J. J.; Lledos, A.; Mereiter, K.; Puerta, M. C.; Valerga, P. *J. Am. Chem. Soc.* **2003**, *125*, 3311–3321. (b) Lomprey, J. R.; Selegue, J. P. *J. Am. Chem. Soc.* **1992**, *114*, 5518–5523.

(8) Allen, F. H. *Acta Crystallogr.* **2002**, *B58*, 380–388.

(9) A Cambridge Structural Database search shows a mean value of 2.108 Å for reported Ru−C(sp^2) bonds in ruthenols. Tot. Obs. = 58, Std. Dev. = 0.054.

(10) (a) Schmid, R.; Kirchner, K. *Eur. J. Inorg. Chem.* **2004**, 2609–2626. (b) Ernst, C.; Walter, O.; Dinjus, E.; Arzberger, S.; Gorls, H. *J. Prak. Chem.* **1999**, *341*, 801–804. (c) Albers, M. O.; Dewaal, D. J. A.; Liles, D. C.; Robinson, D. J.; Singleton, E.; Wiege, M. B. *J. Chem. Soc., Chem. Commun.* **1986**, 1680–1682. (d) Pu, L.; Hasegawa, T.; Parkin, S.; Taube, H. *J. Am. Chem. Soc.* **1992**, *114*, 2712–2713. (e) Hill, A. F.; Rae, A. D.; Schultz, M.; Willis, A. C. *Organometallics* **2007**, *26*, 1325–1338.

(11) (a) Bart, S. C.; Lobkovsky, E.; Chirik, P. J. *J. Am. Chem. Soc.* **2004**, *126*, 13794–13807. (b) Boncella, J. M.; Green, M. L. H.; O'Hare, D. *J. Chem. Soc., Chem. Commun.* **1986**, 618–619. (c) Harris, T. V.; Rathke, J. W.; Muetterties, E. L. *J. Am. Chem. Soc.* **1978**, *100*, 6966–6977.

(12) Mackenzie, K.; Gravett, E. C.; Howard, J. A. K.; Astin, K. B.; Tomlins, A. M. *J. Chem. Soc., Perkin Trans. 2* **1996**, 1240–1241.

(13) Silverstein, R. M.; Webster, F. X. *Spectrometric Identification of Organic Compounds*; John Wiley & Sons: New York, 1998.

(14) Brookhart, M.; Green, M. L. H.; Parkin, G. *Proc. Natl. Acad. Sci. U. S. A.* **2007**, *104*, 6908–6914.

(15) Yoo, H. Ph.D. Thesis, University of Pennsylvania, 2006.

(16) Frisch, M. J. T., G. W.; Schlegel, H. B.; Scuseria, G. E.; Robb, M. A.; Cheeseman, J. R.; Scalmani, G.; Barone, V.; Mennucci, B.; Petersson, G. A.; Nakatsuji, H.; Caricato, M.; Li, X.; Hratchian, H. P.; Izmaylov, A. F.; Bloino, J.; Zheng, G.; Sonnenberg, J. L.; Hada, M.; Ehara, M.; Toyota, K.; Fukuda, R.; Hasegawa, J.; Ishida, M.; Nakajima, T.; Honda, Y.; Kitao, O.; Nakai, H.; Vreven, T.; Montgomery, Jr., J. A.; Peralta, J. E.; Ogliaro, F.; Bearpark, M.; Heyd, J. J.; Brothers, E.; Kudin, K. N.; Staroverov, V. N.; Kobayashi, R.; Normand, J.; Raghavachari, K.; Rendell, A.; Burant, J. C.; Iyengar, S. S.; Tomasi, J.; Cossi, M.; Rega, N.; Millam, N. J.; Klene, M.; Knox, J. E.; Cross, J. B.; Bakken, V.; Adamo, C.; Jaramillo, J.; Gomperts, R.; Stratmann, R. E.; Yazyev, O.; Austin, A. J.; Cammi, R.; Pomelli, C.; Ochterski, J. W.; Martin, R. L.; Morokuma, K.; Zakrzewski, V. G.; Voth, G. A.; Salvador, P.; Dannenberg, J. J.; Dapprich, S.; Daniels, A. D.; Farkas, Ö.; Foresman, J. B.; Ortiz, J. V.; Cioslowski, J.; Fox, D. J. *Gaussian 09*, Revision A.02; Gaussian Inc: Wallingford, CT, 2009.

(17) (a) Becke, A. D. *J. Chem. Phys.* **1986**, *84*, 4524–4529. (b) Lee, C. T.; Tang, W. T.; Parr, R. G. *Phys. Rev. B* **1988**, *37*, 785–789.

(18) Rassolov, V. A.; Ratner, M. A.; Pople, J. A.; Redfern, P. C.; Curtiss, L. A. *J. Comput. Chem.* **2001**, *22*, 976–984.

(19) (a) Küchle, W.; Dolg, M.; Stoll, H.; Preuss, H. *Mol. Phys.* **1991**, *74*, 1245–1263. (b) Dolg, M.; Wedig, U.; Stoll, H.; Preuss, H. *J. Chem. Phys.* **1987**, *86*, 866–872.

(20) Martin, J. M. L.; Sundermann, A. *J. Chem. Phys.* **2001**, *114*, 3408–3420.

(21) (a) Seeger, R.; Pople, J. A. *J. Chem. Phys.* **1977**, *66*, 3045–3050. (b) Schlegel, H. B.; McDouall, J. J. In *Computational Advances in Organic Chemistry*; Ögretir, C., Csizmadia, I. G., Eds.; Kluwer Academic: The Netherlands, 1991. (c) Bauernschmitt, R.; Ahlrichs, R. *J. Chem. Phys.* **1996**, *104*, 9047–9052.

(22) (a) Dewar, M. J. S. *Bull. Soc. Chim. Fr.* **1951**, *18*, C79. (b) Chatt, J.; Duncanson, L. A. *J. Chem. Soc.* **1953**, 2939–2947.

(23) Alt, H. G.; Han, J. S.; Rogers, R. D.; Thewalt, U. *J. Organomet. Chem.* **1993**, *459*, 209–217.

(24) Templeton, J. L.; Ward, B. C. *J. Am. Chem. Soc.* **1980**, *102*, 3288–3290.

(25) (a) Kamata, M.; Hirotsu, K.; Higuchi, T.; Kido, M.; Tatsumi, K.; Yoshida, T.; Otsuka, S. *Inorg. Chem.* **1983**, *22*, 2416–2424. (b) Ishino, H.;

Kuwata, S.; Ishii, Y.; Hidai, M. *Organometallics* **2001**, *20*, 13–15. (c) Ricard, L.; Weiss, R.; Newton, W. E.; Chen, G. J. J.; Mcdonald, J. W. *J. Am. Chem. Soc.* **1978**, *100*, 1318–1320. (d) Kersting, M.; El-Kholi, A.; Muller, U.; Dehnicke, K. *Chem. Ber.* **1989**, *122*, 279. (e) Barrio, P.; Esteruelas, M. A.; Onate, E. *Organometallics* **2003**, *22*, 2472–2485. (f) Ganesan, M.; Shih, K. Y.; Fanwick, P. E.; Walton, R. A. *Inorg. Chem.* **2003**, *42*, 1241–1247. (g) Alt, H. G.; Engelhardt, H. E. *J. Organomet. Chem.* **1988**, *342*, 235. (h) Pörschke, K. R.; Tsay, Y. H.; Kruger, C. *Angew. Chem., Int. Ed. Engl.* **1985**, 323. (i) Pu, L.; Hasegawa, T.; Parkin, S.; Taube, H. *J. Am. Chem. Soc.* **1993**, *115*, 2545–2546. (j) Bullock, R. M. *J. Chem. Soc., Chem. Commun.* **1989**, 165–167. (k) Kowalczyk, J. J.; Arif, A. M.; Gladysz, J. A. *Organometallics* **1991**, *10*, 1079–1088.

(26) Yi, C.; Torres-Lubian, J.; Liu, N.; Rheingold, A.; Guzei, I. *Organometallics* **1998**, *17*, 1257–1259.

(27) Agenet, N.; Gandon, V.; Vollhardt, K. P. C.; Malacria, M.; Aubert, C. *J. Am. Chem. Soc.* **2007**, *129*, 8860–8871.

(28) Kirchner, K.; Calhorda, M. J.; Schmid, R.; Veiros, L. F. *J. Am. Chem. Soc.* **2003**, *125*, 11721–11729.

(29) Yamamoto, Y.; Arakawa, T.; Ogawa, R.; Itoh, K. *J. Am. Chem. Soc.* **2003**, *125*, 12143–12160.

(30) Wayda, A. L.; Darensbourg, M. Y., Eds. *Experimental Organometallic Chemistry*; American Chemical Society: Washington, DC, 1987.

(31) Perrin, D. D.; Armarego, W. L. *Purification of Laboratory Chemicals*; Pergamon Press: New York, 1988.

(32) Luetkens, M. L.; Sattelberger, A. P.; Murray, H. H.; Basil, J. D.; Fackler, J. P. *Inorg. Synth.* **1989**, *26*, 7.

(33) *CrystalClear*; Rigaku Corporation, 1999.

(34) *CrystalStructure*; Rigaku Corporation, 2002.

(35) Altomare, A.; Burla, M. C.; Camalli, M.; Cascarano, G.; Giacovazzo, C.; Guagliardi, A.; Moliterni, A. G. G.; Polidori, G.; R., S. *J. Appl. Crystallogr.* **1999**, *32*, 115–119.

(36) Sheldrick, G. M. *SHELXL-97: Program for the Refinement of Crystal Structures*; University of Göttingen: Göttingen, Germany, 1997.

(37) Sluis, P.; Spek, A. L. *Acta Crystallogr.* **1990**, *A46*, 194.